International Journal of Architectural, Civil and Construction Sciences
ISSN: 2415-1734
Vol:10, No:4, 2016

Analysis of Residual Stresses and Angular Distortion in Stiffened Cylindrical Shell Fillet Welds Using Finite Element Method

M. R. Daneshgar, S. E. Habibi, E. Daneshgar, A. Daneshgar

***Abstract*—**In this paper, a two-dimensional method is developed to simulate the fillet welds in a stiffened cylindrical shell, using finite element method. The stiffener material is aluminum 2519. The thermo-elasto-plastic analysis is used to analyze the thermo-mechanical behavior. Due to the high heat flux rate of the welding process, two uncouple thermal and mechanical analysis are carried out instead of performing a single couple thermo-mechanical simulation. In order to investigate the effects of the welding procedures, two different welding techniques are examined. The resulted residual stresses and distortions due to different welding procedures are obtained. Furthermore, this study employed the technique of element birth and death to simulate the weld filler variation with time in fillet welds. The obtained results are in good agreement with the published experimental and three-dimensional numerical simulation results. Therefore, the proposed 2D modeling technique can effectively give the corresponding results of 3D models. Furthermore, by inspection of the obtained residual hoop and transverse stresses and angular distortions, proper welding procedure is suggested.

Keywords—Stiffened cylindrical shell, fillet welds, residual stress, angular distortion, finite element method.

I. Introduction

NOWADAYS, welding industry is important in constructions and specimen reparations. The types of welded joint can be classified into five basic categories including butt, fillet, corner, lap and edge welds [1]. It is well known phenomenon that due to the localized heating and the subsequent rapid cooling, residual stresses appear around welding zones and cause post-weld deformations of the structure [2]. Fillet weld is the most common weld type used in the fabrication of structural elements in shipbuilding, automobile and other industries. Fillet-welded joints usually suffer from various welding deformation patterns, such as longitudinal and transverse shrinkage, angular distortion and flexural bending. Welding deformation has negative effects on the fabrication accuracy, external appearance and various strengths of the welded structures [3].

M. R. Daneshgar is with the Department of Mechanical Engineering, Persian Gulf University, Boushehr, Iran (Coresponding author; phone: +989174010017; e-mail: Daneshgar.heat@yahoo.com).

S. E. Habibi and E. Daneshgar are with the Department of Mechanical Engineering, Persian Gulf University, Boushehr, Iran (e-mail: Habibie@pgu.ac.ir, Ehsan.daneshgar@gmail.com).

A. Daneshgar is with the Department of Mechanical Engineering, Amirkabir University of Technology, Tehran, Iran (e-mail: Amin.daneshgar@aut.ac.ir).

Many authors have theoretically and experimentally tried to predict the residual stresses and deformations in welding connections [4]-[9]. The complex nature of the welding process causes some difficulties in analyzing and numerical modeling methods. The sources of complexities include temperature related material and thermal properties, transient heat transfer with complicated boundary conditions, moving heat sources, phase changes and transformations, complex residual stress states and the difficulties of making experimental measurements at high temperatures [10].

Generally speaking, a finite element simulation of the welding process consists of two main parts: the thermal analysis and the mechanical stress analysis [3], [11]-[14]. Finite element simulation as a trusted method has been employed at an increasing rate for simulation of the welding process [15], [16]. Many researchers have utilized the commercial finite element code ABAQUS, expanded with user subroutines, to model welding process simulations with great success [6], [17]-[21]. The finite element code ADINAT was used by [22], while other authors [23]-[25] have utilized SYSWELD to perform weld simulations. To reduce the computational costs of the simulation, many solutions are suggested by the authors. In the case of 3D numerical analysis, it is always recommended to use symmetry conditions [1], [12], [14]. In some studies, 3D models are replaced by 2D models [1], [19], [24], [26]-[28]. Furthermore, complicated heat flux forms usually are replaced with a uniform one [29], [30] or sometimes thermal and mechanical analysis may be performed separately (uncoupled thermo-mechanical finite element analyses) [3], [31]-[33]. Furthermore, thermal boundary conditions can also be simplified for example convection and radiation coefficients may be assumed as constant values [19], [20]. To further simplify the model, there are also alternative solutions such as the inherent strain method [18].

Dubois et al. [24] have utilized 2D models, in contrast with the recognition that the 3D effect of the movement of the electrode has been neglected. Hong et al. [19] dispute the need for 3D weld models, suggested that a 2D analysis can be carried out with appropriate simplifying assumptions depending on the nature of the problem. Barsoum et al. [28] showed that, a main objective in employing 2D simulation is the significant reduction in the computational time (CPU time). Furthermore, they also showed that the residual stress predictions in the 2D simulation model show a good agreement with the measurement values.

Shim et al. [30] used ramp function to model the arc motion when the arc approaches, travels across and departs from the specified cross section. Vakili et al. [34] used the Double-Ellipsoidal Heat Source (DEHS) model previously proposed by [35]. He modified the model by introducing a new set of coefficients to simulate fillet weld joint. Then, the extended model is implemented into a finite element code in which 2D and 3D temperature and deformation fields in the weldment can be obtained. He is asserted that 2D model can only be used in the thermal analysis provided that a new term, which simulates the movement of the heat source, has been added to the formulation.

Several authors have tried to answer that whether it is necessary to perform the couple thermo-mechanical analysis or the same accuracy level can be achieved by the simpler uncouple analysis [17], [22], [24], [25], [31], [33], [36]-[38]. Oddy et al. [31], [32] state the heat generated by the plastic deformation is much less than the heat introduced by the weld arc itself. Therefore, the thermal analysis may be performed separately from the mechanical analysis. Chang and Lee [33] performed 3D uncoupled thermo-mechanical finite element analysis of the residual stresses in the T-joint fillet welds made from similar and dissimilar steels. Zaeem et al. [39] showed that the decoupling of the thermal analysis from the mechanical analysis and using Anand constitutive equations for elastic–viscoplastic behaviors of welded structure reduces the computational time and cost without noticeably decreasing the accuracy of results. Dean Deng et al. [3] showed that the thermo-mechanical behavior can be simulated using uncoupled formulation. They notice that due to the negligible dimensional change in welding process, the internal strain energy is insignificant compared with the thermal energy imposed from the welding heat source. Therefore, they solved the heat transfer problem independently to obtain temperature distribution history. Afterward, the computed temperature history was employed as a thermal load in the subsequent mechanical analysis with the temperature-dependent thermo-mechanical properties.

To model the heat exchange with the environment in the finite element model, surface or skin elements are typically used [22], [31]. Michaleris et al. [26] used radiation and convection boundary conditions for all free surfaces in the thermal analyses through the use of a temperature dependent convection coefficient. Hong et al. [19] use a similar approach by specifying a single heat loss coefficient for all surfaces. Brown and Song [20] incorporate convective heat transfer. They assumed that the coefficients depend both on the temperature and the orientation of the boundary. They have been modeled radiation by the standard Boltzmann relation and it is assumed that the radiation is occurred from the free surfaces to ambient air only. Nonetheless, the effect of radiation is typically smaller than the effect of convection except near the melting temperature.

This paper is going to present a method for analyzing the 3D welding process using a 2D simulation technique. To show the applicability of the method, a common welding problem with numerous industrial applications is considered. With the help of some properly defined thermal and mechanical boundary conditions, 2D simulation results which can effectively predict the 3D simulation results were obtained. We have also investigated the effects of different welding techniques. In the first technique, both the left and the right weld paths are implemented simultaneously and in the second method, the second weld path is performed after the first one is cooled down.

II. Analysis of Model

A. Thermo-Mechanical Model

1. Thermal Model

The method which is used in applying the heat flux plays a significant role in the welding analysis. In this paper, heat flux is gradually applied to the model using a ramp function and after a period of constant flux, the heat flux is decreased gradually according to the second ramp function. Shim et al [30] used the ramp heat input model to avoid numerical convergence problems due to an instantaneous increase in temperature near the fusion zone and to include the effect of a moving arc in the weld plane (1). Fig. 1 shows the flux as a function of time for a general ramp input model.

$$t_1 = t_3 = \%20 \times (t_1 + t_2) \tag{1}$$

The amount of the heat input is the product of arc the efficiency (η), voltage (V) and the current (I). The total heat flux is uniformly imposed to the weld metal. The heat source power can be considered as

$$Q = \eta VI \tag{2}$$

We assume $\eta = 0.88$ which is also used in the reference [40]. The other welding parameters are I=20 A, V=250 v, welding speed v=6 mm.sec^{-1} and welding procedure is single pass arc welding. Accordingly, Q is 4.8 KW.

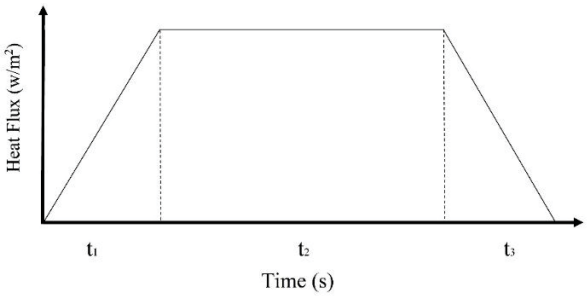

t_1: initial ramp time

t_2: maximum input time

t_3: decaying ramp time

Fig. 1 General Shape for the Ramp Model [30]

It is shown that the weld arc diameter can be considered approximately 11 mm [40]. Therefore, the maximum heat flux

at the heat affected zone during the welding process with the assumed circular molten zone can be calculated as

$$q'' = \frac{Q}{A} = \frac{4800}{\pi \times (11 \times 10^{-3})^2} = 125 \times 10^5 \ (\frac{w}{m^2}) \quad (3)$$

The free surfaces are considered as exposed ones. The effective combined convection and radiation coefficient is considered as $10 W/m°C$ [40].

2. Mechanical Model

The temperature history obtained from the thermal analysis is imposed on the structural model as a thermal load. The thermal strains and stresses can be calculated at each time increment. Also, the final state of residual stresses will be worked out from the thermal strains and stresses. The residual stresses from each temperature are imposed on the model to determine the updated behavior of the model before the next temperature increment. Volume changes due to the phase transition were neglected. The material was assumed to follow the Von Misses yield criterion and the associated flow rules.

B. Element Birth and Death

To simulate the weld filler variation with the time in fillet welds, the element birth and death technique is utilized. Elements representing each weld pass were initially removed and reactivated for each pass to simulate the deposition of the weld beads. Then, the heat flux is applied to these newly activated elements as the imposed heat load.

C. Analysis Procedure

During the welding process thermal stresses are calculated from the temperature distributions which in turn were previously determined by the thermal analysis. The residual stresses in each temperature increment are imposed on the model to determine the updated behavior of the model before the next temperature increment. This method is also used previously in [1]. The same finite element mesh and time increments were used for both thermal and structural analysis. While the static analysis can be adopted for the stress analysis, the thermal analysis should be carried out using transient modeling technique to trace the rapid change of temperature with the time. However, a significant number of time points, at which the temperature results are to be read into the stress analysis, should be defined properly to capture the temperature gradient and to give accurate residual stresses.

D. Material Properties

The Aluminum-2519 is used as the base metal with the temperature dependent thermal and the mechanical properties as shown in Fig. 2. The base metal is assumed as incompressible material with the density of 2823 (Kg/m^3). the Poison coefficient is considered as 0.334.

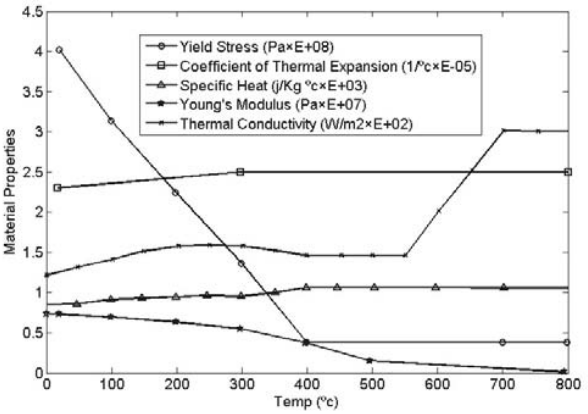

Fig. 2 Thermal and the mechanical properties of an aluminum-2519

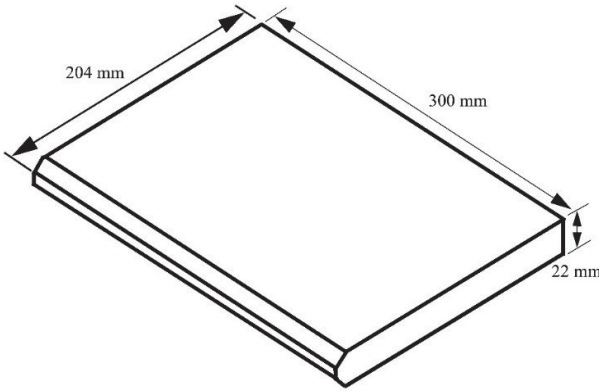

(a) Plate dimensions

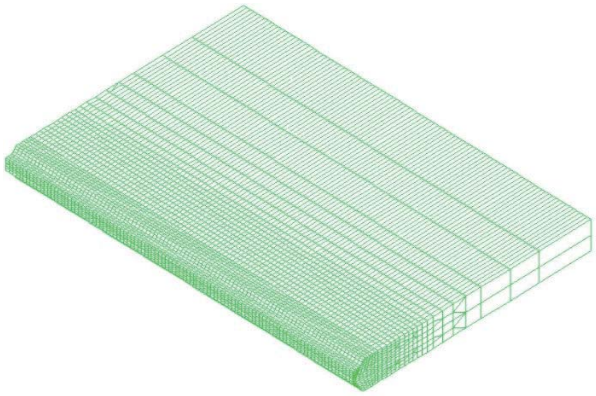

(b) 3D finite element mesh

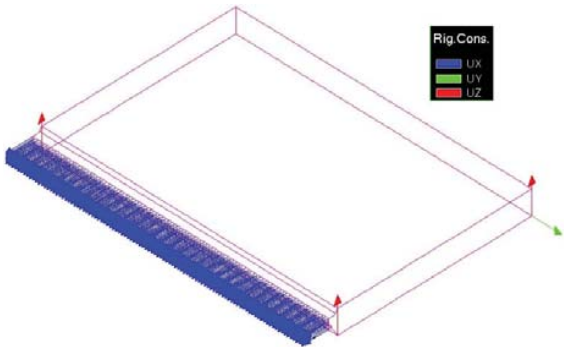

(c) Mechanical constraints for butt joint

Fig. 3 The aluminum-2519 plates [42]

E. Verification

To verify the proposed method, the results are compared with the corresponding ones obtained via 3D finite element modeling of butt welding process in welding of the two aluminum-2519 plates reported in [40]. The plate dimensions, the plate 3D finite element model and the mechanical constraints on the half model are shown in Fig. 3. Since the plate thicknesses are greater than 13 mm for this butt joint model, it is a design recommendation that the plates be chamfered in a double v-groove configuration along the joint as can be seen in this figure. The mid-plane of the root gap is assumed to be the plane of symmetry in the analysis, So the half model is analysed. Due to the symmetry condition, the model is fixed along the normal to the symmetry axis. Fig. 3 (c) depicts the specified zero displacement conditions for the butt joint. This butt joint model is similar to the model which have been studied by Michaleris et al. [41], except for the elimination of the run-off tabs. Michaleris investigated the six pass aluminum weld joint to determine the effects of restraint in the formation of welding distortion. The focus of reference [41] is to determine the residual stress state in the part of the model where the "steady state" of the welding process has been attained.

The corresponding proposed 2D Finite element model of this problem is shown in Fig. 4. because of the high temperature gradient around the welding zone, a very fine mesh is used.

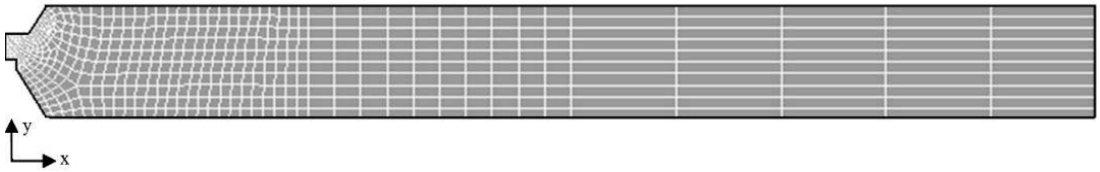

Fig. 4 Plate 2D finite element mesh

The v-groove boundary is subjected to the arc welding, so the thermal boundary condition is considered as a heat flux (q_s''). Due to the symmetry of the problem with respect to the Y axis, the isothermal thermal boundary condition is applied. Convection and radiation boundary conditions are imposed on the other external boundaries. The model is fixed in the longitudinal X direction at the symmetry Y axis. These assumptions cause somewhat higher stresses values during the welding process.

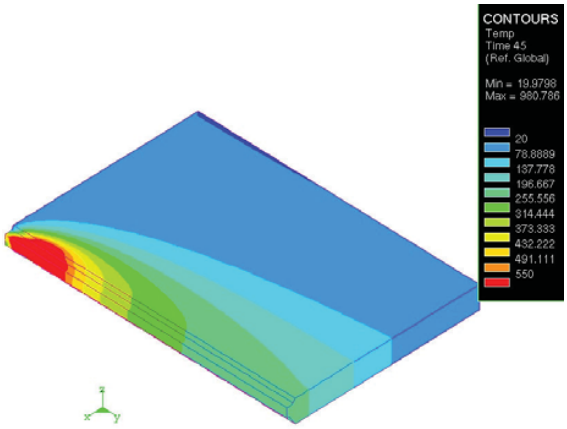

(a) Surface temperature distribution during the first weld pass of the butt joint model at t = 45s

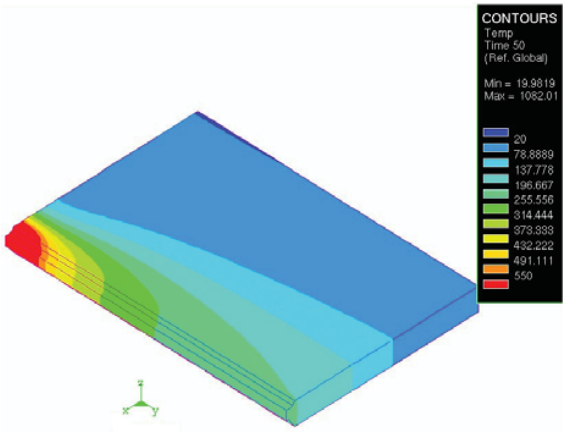

(b) Surface temperature distribution during the first weld pass of the butt joint model at t = 50s

Fig. 5 Surface temperature distribution during the first weld pass of the butt joint model at t = 45 and 50s [42]

Fig. 5 shows surface temperature distribution during the first weld pass of the butt joint model at t = 45 and 50s [40] and Fig. 6 shows thermal history at two critical points A and B from 2D analysis.

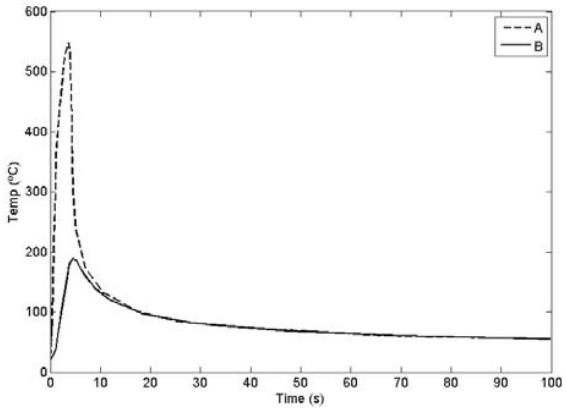

(a) Plate thermal history at two critical points A and B

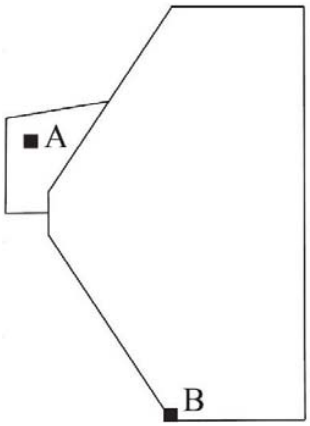

(b) Place of two critical points A and B

Fig. 6 Plate thermal history resulted from the proposed 2D analysis

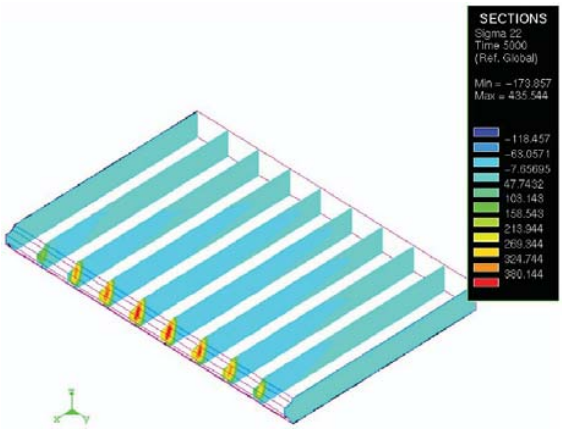

Fig. 7 Longitudinal residual stress 3D contour [42]

The results of 3D finite element simulation show that the maximum temperature of the plate during the welding process is 550ºc. The 2D analysis, has predicted this as 555ºc. Fig. 7 shows the longitudinal residual stress contour obtained in [39]. According to this figure, maximum residual stress is equal to 435 Mpa. Residual stress distribution obtained from 2D analysis is shown in Fig. 8.

Maximum residual stress is predicted 420Mpa. So, this method has approximately 3% error with Justin D. Francis method. Fig. 9 shows the longitudinal residual stress distribution induced by the welding process on the top of the 2D plate.

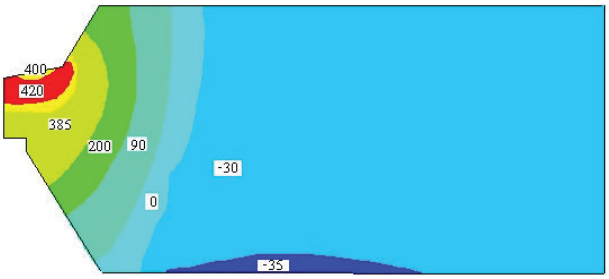

(a) Residual stress contour of critical points

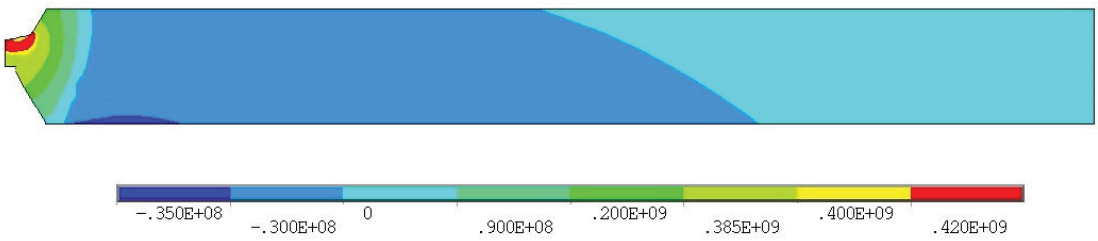

(b) Residual stress contour of total plate

Fig. 8 Residual stress contour taken from 2D analysis

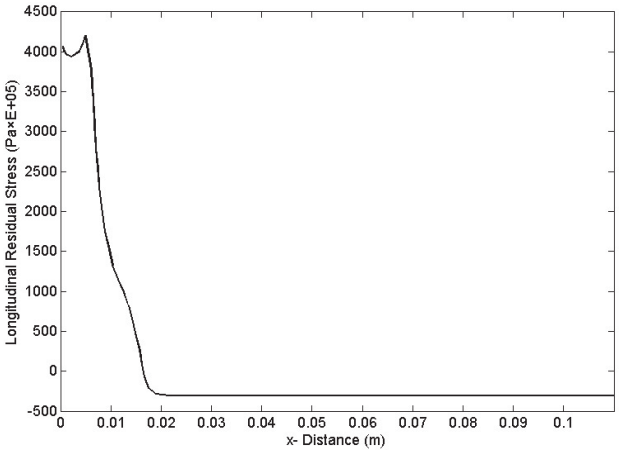

Fig. 9 Longitudinal residual stress distribution resulted from 2D analysis

Accordingly, the present two dimensional modeling technique can effectively give the results of the three dimensional finite element modeling.

III. Analysis of the Fillet Weld

A. Stiffener Geometry

Fig. 10 depicts the stiffener geometry. In this figure, Y-direction is the circumferential axisymmetric axis of the stiffened cylindrical shell.

In Fig. 11 (a) complete geometry of the stiffened cylindrical shell and in Figs. 11 (b) and (c), sectioned stiffened cylindrical shell are shown.

As a result of axisymmetric condition, the entire displacement component in X-direction is zeroed. Furthermore, due to the far distance from the heat affected zone and the axisymmetric condition, the two extreme sides of the model is fixed (Fig. 12).

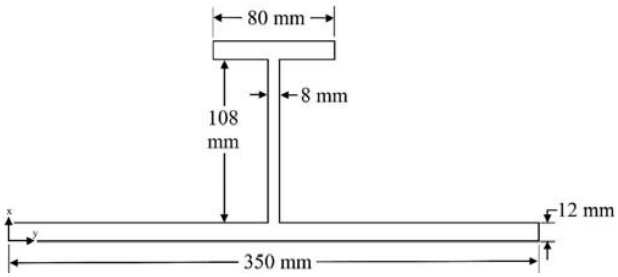

Fig. 10 Stiffener geometry

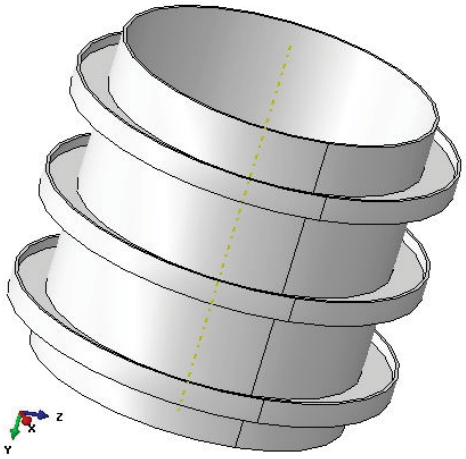

(a) Complete stiffened cylindrical shell

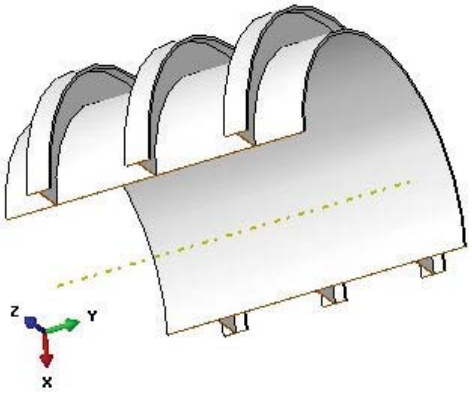

(b) Sectioned stiffened cylindrical shell

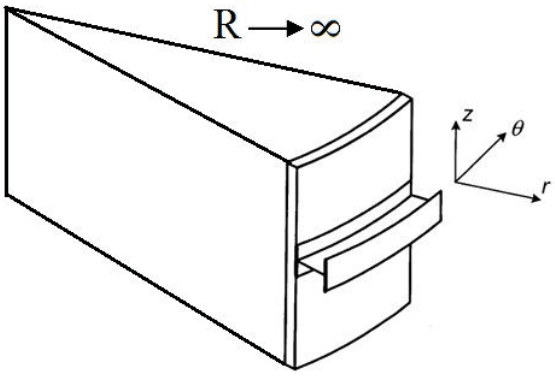

(c) Sectioned stiffened cylindrical shell in polar coordinate

Fig. 11 The stiffened cylindrical shell

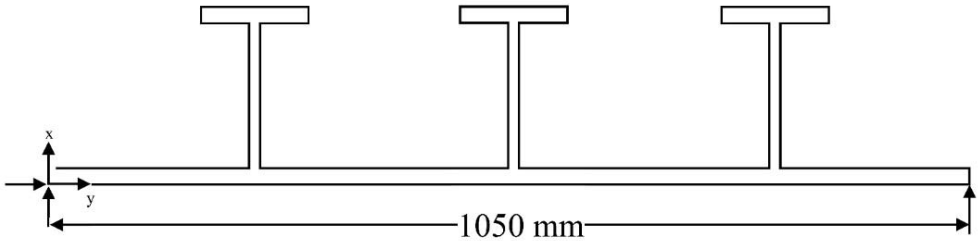

Fig. 12 Mechanical Boundary Conditions of the Stiffener

B. Stiffener Finite Element Model

In Fig. 13 (a), finite element mesh model for middle stiffener and in Fig. 13 (b), finite element mesh model for three continuous stiffeners are shown. Mesh densities has great effects on the results accuracy, so we use a dense fine mesh around the welding zone.

C. Mesh Study

To examine the sensitivity of the results with respect to the element sizes, the effect of mesh refinement was studied. It is shown that considering 620 elements and 700 nodes can adequately give accurate results.

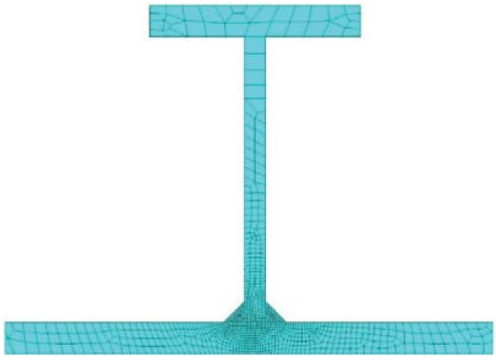

(a) Middle stiffener finite element mesh

(b) Finite element mesh model for three continuous stiffener

Fig. 13 Stiffener finite element mesh

IV. Results

For the welding of the stiffened cylinder, two welding methods are suggested. In the first technique, both the left and the right weld paths are implemented simultaneously and in the second method, the second weld path is performed after the first one is cooled down. Rest time for all welding methods is considered 250s.

A. First Method

In the first method, thermal history at two points A and B, as functions of the to the welding time is shown in Fig. 14.

Hoop and residual transverse stresses for inner and outer surfaces of the cylindrical sheet as functions of the Y-Distance are shown in Figs. 15 (a) and (b), respectively. (Y= $\frac{y}{350}(\frac{\text{mm}}{\text{mm}})$)

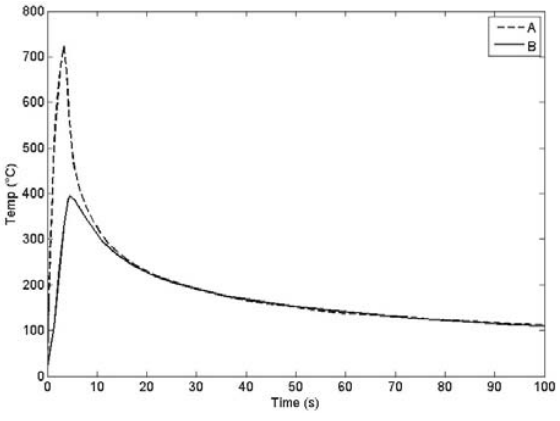

(a) Thermal history at two points A and B in first method

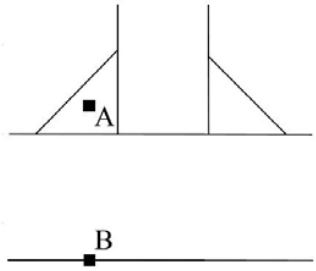

(b) Place of two critical points A and B

Fig. 14 Thermal history at two points A and B in first method taken from 2D analysis

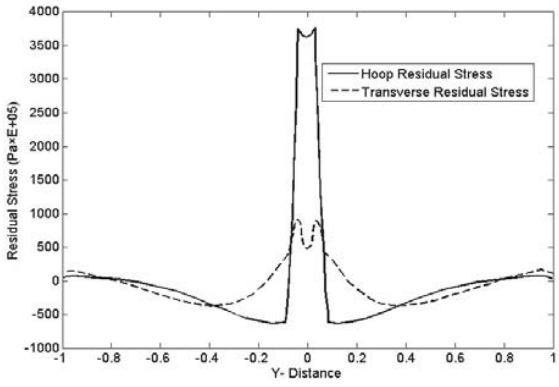

(a) Hoop and residual transverse stress distribution on the inner surface in first method

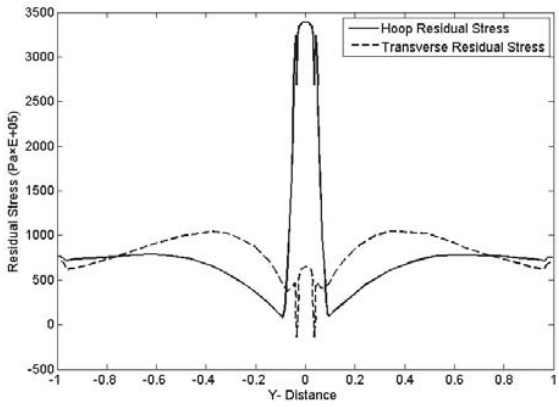

(b) Hoop and residual transverse stress distribution on the outer surface in first method

Fig. 15 Hoop and residual transverse stress distribution in the first method

To analyse the angular distortion of the stiffened cylinder, the angular deformation of the shell is shown by $\Delta\theta$ (Fig. 16). The change of angular distortion in cooling period as a function of time for the first welding method is presented in Fig. 17. This figure reveals that in the first 2s, the heat affected region of cylinder distort in the negative θ-direction (approximately about -0.0044 Rad). This is due to the fact that the thermal expansion in the upper portion exceeds that in the lower one. Afterward, the distortion increased and finally become positive at t=25s. Fig. 17 reveals that, after 140 s of weldment cooling, the angular distortion increase even more (about 0.006 Rad), and thereafter almost does not change. This is because of the upwards bend of the shell due to plastic deformation in the upper portion exceeds that in the lower portion [1].

Angular distortion contour on the deformed shape are shown in Fig. 18.

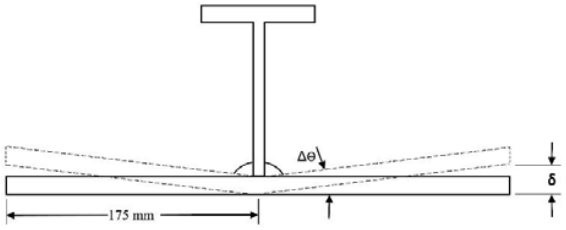

Fig. 16 Angular distortion in the stiffened cylinder

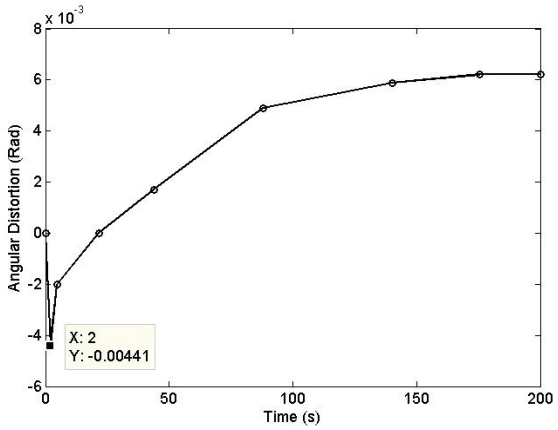

Fig. 17 Change of angular distortion with cooling time in the first method

B. Second Method

In the second method, thermal history at two points A and B, as functions of the welding time, in first and second step are shown in Fig. 19.

Hoop and residual transverse stresses of the stiffener for this method are shown in Figs. 20 (a) and (b), respectively.

Variation of the angular distortion in two cooling period as a function of time for the second method is presented in Fig. 21. Just similar to the first method, in the first 2s, the heat affected region of cylinder is distorted in the negative θ-direction and after the 2s, increases in the positive θ-direction. After the first cooling period (250 sec), the second welding process is performed. Again, the heat affected region is distorted in the negative θ-direction. After second cooling period (500 sec), the final angular distortion is approximately 0.0029 Rad.

Fig. 22 shows that, in the second method in addition to the deformations which are occur in the shell, the web is distorted too. These extra deformations are caused by nonsymmetrical welding process.

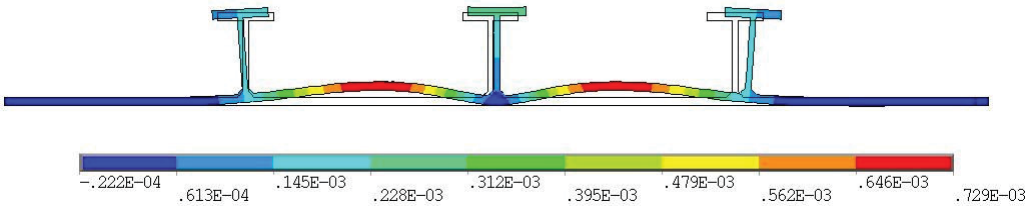

(a) Angular distortion contour in the stiffened cylinder in the first method

(b) Schematic view of the Angular distortion in the stiffened cylinder in the first method

Fig. 18 Angular distortion in the stiffened cylinder in the first method

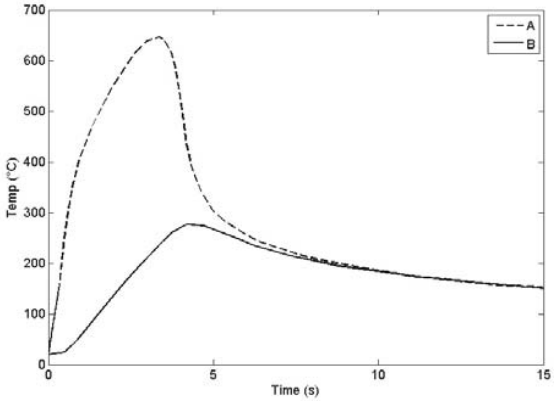

(a) In the first welding pass

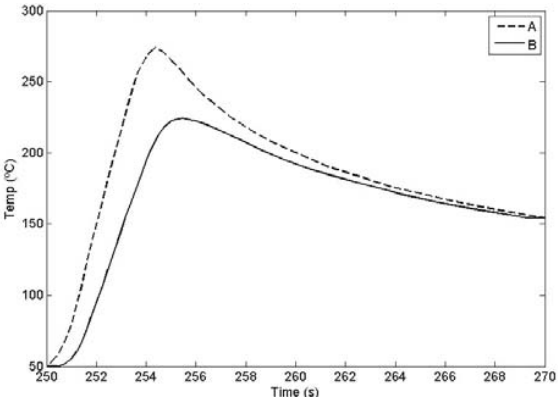

(b) In the second welding pass

Fig. 19 Thermal history in the second method

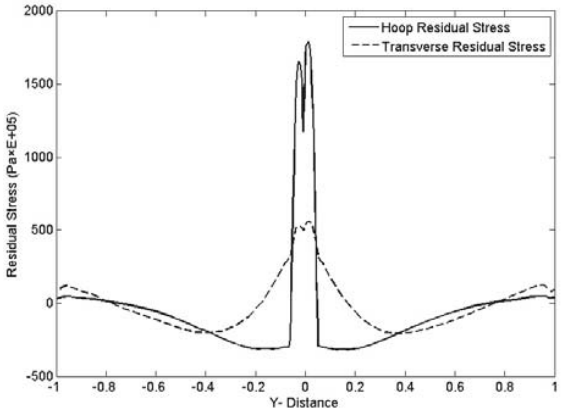

(a) Hoop and residual transverse stress distribution on the inner surface in the second method

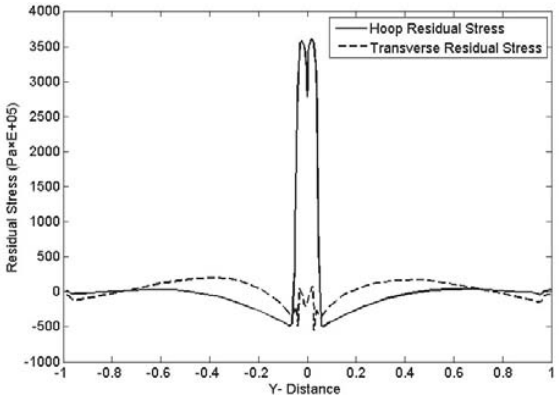

(b) Hoop and residual transverse stress distribution on the outer surface in the second method

Fig. 20 Hoop and residual transverse stress distribution in the second method

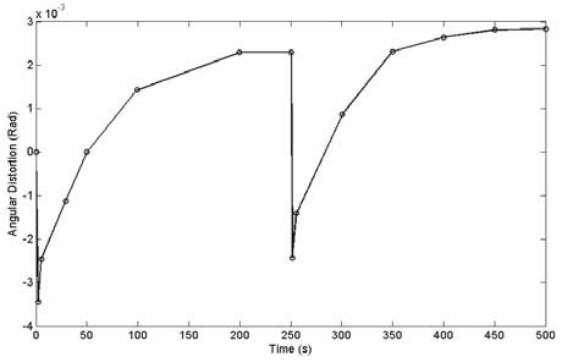

Fig. 21 Variations of angular distortion with respect to the cooling time

V. Discussions

For residual hoop stresses on the inner and the outer surfaces of the stiffened cylindrical shell, the maximum tensile stresses occur near the weld toe, and a compressive stress appears away from the weld toe. For the first method, maximum residual hoop stress occurs on the inner surface of the cylindrical shell. But for the second method, it occurs on the outer surface of the cylindrical shell. This is due to increase of applied heat flux and increase of heat affected zone in the first method.

By comparing the residual hoop stress results, it is clearly known that the first welding method applies higher residual hoop stress on the stiffened cylindrical shell compared with the second one.

For residual transverse stresses on inner surface, a tensile stress is produced near the fillet toe. As the distance from the weld toe increases the compressive stress appears. On the outer surface, compressive stress occurs near the fillet weld toe and tensile stress appears away from the weld toe. It can be clearly seen that the first method applies higher transverse stress on the cylindrical sheet.

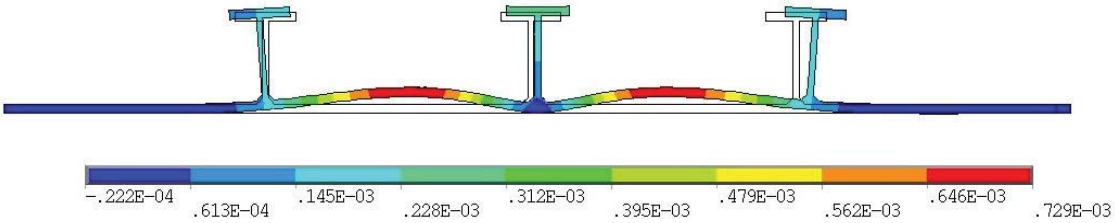

(a) Angular distortion contour in the stiffened cylinder in the second method

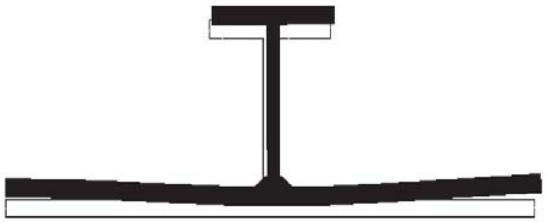

(b) Schematic view of the angular distortion in the stiffened cylinder in the second method

Fig. 22 Angular distortion in the stiffened cylinder in the second method

VI. Conclusions

In this study, a 2D axisymmetric method is developed to simulate the fillet welds of stiffened cylindrical shell, using finite element method. The technique of element birth and death is used to simulate the weld filler variations with time in fillet welds.

For verification purpose, the proposed method was compared with 3D finite element results for the butt joint in aluminum-2519 plates given in [40].

For stiffener analysis, two welding methods were assumed and then residual stress values for these methods were obtained. In the first technique, both the left and the right weld paths are implemented simultaneously and in the second method, the second weld path is performed after the first one is cooled down. Results are in a good agreement with the residual stresses and distortion results obtained in other published experimental and numerical 3D simulations. The thermal elastic plastic finite element model can effectively be employed to predict welding deformation. For larger models, much time saving will be expected by the present procedure.

Comparison of the distortion of the cylindrical shell illustrates that the first method imposed higher distortion than the second method. So, “the second method” is recommended for welding of stiffener because of the lower residual stress values and distortion induced in the cylindrical shell.

REFERENCES

[1] Teng T.L., Fung C.P., Chang P.H. Yang W.C., Analysis of residual stresses and distortions in T-joint fillet welds, J. of int. pressure vessels and piping 78: 523-538, 2001.
[2] Perić M., Tonkovic´ Z., Rodic´ A., Surjak M., Garašic´ I., I. Boras A. Švaic´ S., Numerical analysis and experimental investigation of welding residual stresses and distortions in a T-joint fillet weld, Mat. & Des.; 53: 1052–1063, 2014.
[3] D. Deng W.L., H. Murakawa, Determination of welding deformation in fillet-welded joint by means of numerical simulation and comparison with experimental measurements, J. Mater. Process. Technol.; 183(2–3): 219–225, 2007.
[4] Watanabe M. Satoh K., Effect of welding condition on the shrinkage distortion in welded structures, Weld. J., Weld. Res. Suppl.: 337-384, 1961.
[5] White J.D., Leggatt R.H. Dwight J.B., Weld shrinkage prediction, Weld. Met. Fabrication: 587–596, 1980.
[6] Satoh K. Terasaki T., Effect of welding condition on welding deformation in welded structural materials, J. Jpn. Weld. Soc.; 45(4): 302–308, 1976.
[7] Shibahara M. Murakawa H., Effect of various factors on transverse shrinkage under butt welding, Trans. JWRI; 27 (2): 97–106, 1998.
[8] Tsirkas S.A., Papanikos P. Kermanidis T., Numerical simulation of the laser welding process in butt-joint specimens, J. Mater. Process. Technol.; 134(1): 59–69, 2003.
[9] Verhaeghe G., Predictive Formulate for Weld Distortion—A Critical Review, Abington Publishing, Cambridge, England: 1999.
[10] Boyles L.G., Computer Analysis of Failure Modes in Welded Joints, ASME PVPWeld Residual Stress and Plastic Deformation; 173: 1-4, 1989.
[11] Lee C. Chang K., Three-dimensional finite element simulation of residual stresses in circumferential welds of steel pipe diameter effects, Mater Sci Eng A; 487(21): 0-8, 2008.
[12] Deng D., FEM prediction of welding residual stress and distortion in carbonsteel considering phase transformation effects, Mat. & Des.; 30(5): 59-66, 2009.
[13] Gannon L., Liu Y., Pegg N. Smith M., Effect of welding sequence on residual stressand distortion in flat-bar stiffened plates, Mar. Struct.; 23: 385–404, 2010.
[14] Long H., Gery D., Carlier A. Maropoulos P.G., Prediction of welding distortion inbutt joint of thin plates, Mat. & Des.; 30(41): 26–35, 2009.
[15] Chang P.H..Teng T.L., Numerical and experimental investigation on the residual stress of the butt-welded joints, J. of Comp. Mat. Sci.; 29: 511-522, 2004.
[16] Bonifaz E.A., Finite Element Analysis of Heat Flow in Single-Pass Arc Welds, Weld. J., Weld. res. Supp.; 125: 2003.
[17] Preston R., Smith S., Shercliff H. Withers P., An Investigation into the Residual Stresses in an Aluminum 2024 Test Weld, ASME PVP-Fracture, Fatigue and Weld Residual Stress; 393: 265-277, 1999.
[18] [18] Dong P., Hong J., Bynum J. Rogers P., Analysis of Residual Stresses in Al-Li Alloy Repair Welds, ASME PVP- Approximate Methods in the Design and Analysis of Pressure: 1997.
[19] Hong J.K., Tsai C.L. Dong P., Assessment of Numerical Procedures for Residual Stress Analysis of Multipass Welds, Weld. J., Weld. Res. Suppl.: 372- 382, 1998.
[20] Brown S. Song H., Finite Element Simulation of Welding of Large Structures, ASME Journal of Engineering for Industry; 114: 441-451, 1992.
[21] Dong P., Ghadiali P.N..Brust F.W., Residual Stress Analysis of a Multi-Pass Girth Weld, ASME PVP- Fatigue, Fracture, and Residual Stresses; 373: 421-431, 1998.
[22] Karlsson R.I..Josefson B.L., Three-Dimensional Finite Element Analysis of Temperatures and Stresses in a Single-Pass Butt-Welded Pipe, ASME Journal of Pressure Vessel Technology; 112: 76-84, 1990.
[23] Al. Y.V.E., On the Validation of the Models Related to the Prevision of the HAZ Behaviour, ASME PVP Fracture, Fatigue and Weld Residual Stress; 393: 193-200, 1999.
[24] Dubois D., Devaux J. Leblond J.B., Numerical Simulation of a Welding Operation: Calculation of Residual Stresses and Hydrogen Diffusion, ASME Fifth International Conference on Pressure Vessel Technology, Materials and Manufacturing; 2: 1210 - 1238., 1984.
[25] Junek L., Slovacek M., Magula V. Ochodek V., Residual Stress Simulation Incorporating Weld HAZ Microstructure, ASME PVP-Fracture, Fatigue and Weld Residual Stress; 393: 179-192, 1999.
[26] Michaleris P. Debicciari A., Prediction of welding distortion, Weld. J., Weld. Res. Suppl.; 76(4): 172-180, 1997.
[27] Deo M.V., Michaleris P. Sun J., Prediction of buckling distortion of welded structures, Sci. Technol. Weld. Join.; 8: 55-61, 2003.
[28] Barsoum Z. Lundbäck A., Simplified FE welding simulation of fillet welds - 3D effects on the formation residual stresses, Eng. Fail. Analysis; 16(7): 2281-2289, 2009.
[29] Pilipenko A., Computer simulation of residual stress and distortion of thick plates in multi-electrode submerged arc welding, Doctoral Thesis,: 2001.
[30] Shim Y., Feng Z., Lee S., Kim D., Jaeger J., Papitan J.C. C.L. Tsai, Determination of Residual Stress in Thick-Section Weldments, Weld. J., Weld. Res. Suppl.: 305-312, 1992.
[31] Oddy A.S., Goldak J.A..McDill J.M.J., Transformation Plasticity and Residual Stresses in Single-Pass Repair Welds, ASME PVP- Weld Residual Stresses and Plastic Deformation; 173: 13-18, 1989.
[32] Oddy A.S., McDill J.M.J..Goldak J.A., Consistent strain fields in 3D FE analysis of Welds, ASME Journal of Pressure Vessel Technology; 112: 309-311, 1990.
[33] Chang K. Lee C., Finite element analysis of the residual stresses in T-joint fillet welds made of similar and dissimilar steels, Int. J. Adv. Manuf. Technol.; 41(250): 2009.
[34] Vakili-Tahami F. Ziaei-Asl A., Numerical and experimental investigation of T-shape fillet welding of AISI 304 stainless steel plates, Mat. & Des.; 47: 615-623, 2013.
[35] Goldak J., Chakravarti A. Bibby M.A., New finite element model for heat sources, Metall Trans B; 15: 299-305, 1984.
[36] Karlsson L., Jonsson M., Lindgren L.E., Nasstrom M. Troive L., Residual Stresses and Deformations in a Welded Thin-walled Pipe, ASME PVP- Weld Residual Stress and Plastic Deformation; 173: 7-10, 1989.
[37] Michaleris P., Dantzig J.D. Tortorelli, Minimization of Welding Residual Stress and Distortion in Large Structures, Weld. J., Weld. Res. Suppl.: 361-366, 1999.
[38] Chao Y. Qi X., Thermo-mechanical Modeling of Residual Stress and Distortion During Welding Process, ASME PVP- Fracture, Fatigue and Weld Residual Stress; 393: 209-213, 1999.
[39] Zaeem M.A., Nami M.R. Kadivar M.H., Prediction of welding buckling distortion in a thin wall aluminum T join, Comp. Mat. Sci.; 38(4): 588-594, 2007.
[40] Francis J.D., Welding Simulations of Aluminum Alloy Joints by Finite Element Analysis, Virginia Polytechnic University; M.Sc.: 2002.
[41] Michaleris P., Feng Z. Campbell G., Evaluation of 2D and 3D FEA Models for Predicting Residual Stress and Distortion, ASME PVP-Approximate Methods in the Design and Analysis of Pressure Vessels and Piping Components; 347: 91-102, 1997.
[42] Francis J.D., Welding Simulations of Aluminum Alloy Joints by Finite Element Analysis, M.Sc.: 2002.